

ANALYTIC COMPACT MODEL of BALLISTIC and QUASI-BALLISTIC CYLINDRICAL GATE-ALL-AROUND MOSFET INCLUDING TWO SUBBANDS

He CHENG^{1,2}, Shigeyasu UNO^{2,3}, Tatsuhiro NUMATA^{1,2}, Kazuo NAKAZATO¹

¹⁾ *Department of Electrical Engineering and Computer Science, Graduate School of Engineering, Nagoya University, Furo-cho, Chikusa-ku, Nagoya 464-8603, Japan*

²⁾ *JST, CREST, 5 Sanban-cho, Chiyoda-ku, Tokyo 102-0075, Japan*

³⁾ *Department of Electrical and Electronic Engineering, Ritsumeikan University, 1-1-1 Noji-Higashi, Kusatsu, Shiga, 525-8577, Japan*

E-mail: cheng.he@echo.nuee.nagoya-u.ac.jp, suno@fc.ritsumei.ac.jp

INTRODUCTION

Gate-All-Around (GAA)-MOSFETs have been attracting ever-increasing attention, and quantum mechanics and ballistic transport effects have been introduced to study their properties. Although the numerical calculations of model of drain current can be evaluated quite accurately, it takes an immense amount of time, so it is practically impossible to be used in a circuit-level simulation. To overcome this issue, a compact model expressing drain current with one analytic formula in all operating regions is required. Until now, some fully analytic compact models have been reported, but only the lowest subband is considered^[1,2,3]. More than one subband must be considered to maintain good accuracy, when wire radius becomes larger than 1.5nm^[4]. In this work, we propose a compact model incorporating two subbands for the first time, which provides one analytic formula of drain current for all operating regions.

CALCULATION METHOD

Numerical Method

Figure 1 summarizes the idealized structure of one GAA-MOSFET with cylindrical cross section. Electrons are injected from the source into the channel across a potential barrier whose height is modulated by gate voltage. Figure 2(a) schematically shows potential profiles in the channel region. Here the potential profile in cross section of channel can be approximated as a parabolic function along radius direction^[2](Figure 2(b)). Both surface potential and the confinement energy levels (which are above the top of potential barrier along the channel) in cross section of channel are functions of ΔU_G ^[2], an unknown parameter representing potential difference between center of channel and surface along radius direction. Hence ΔU_G can be calculated numerically by coupling equations of Gauss' law and quantum statistics as follows:

$$4\pi\epsilon_{\text{ch}}\Delta U_G = e\sqrt{\frac{k_B T m_c^*}{2\pi^2 \hbar^2}} \times \sum_{n_v} \sum_{n_\phi} \sum_{n_r} g_{n_v} \left[\begin{aligned} & (1+R_{\text{ref}})F_{-1/2} \left(\frac{w_s(\Delta U_G)}{V_t} - \frac{E_{n_\phi, n_r}^q(\Delta U_G)}{k_B T} \right) \\ & + (1-R_{\text{ref}})F_{-1/2} \left(\frac{w_s(\Delta U_G)}{V_t} - \frac{E_{n_\phi, n_r}^q(\Delta U_G)}{k_B T} - \frac{V_{\text{DS}}}{V_t} \right) \end{aligned} \right], \quad (1)$$

where g_{n_v} is degeneracy of valleys, ϵ_{ch} is dielectric constant of channel, m_c^* is the effective mass, corresponding to the transport direction, E_{n_ϕ, n_r}^q is confinement energy level (with respect to surface potential w_s), n_r is the radial quantum number, n_ϕ is the angle quantum number, V_{DS} is the

drain voltage, R_{ref} is the reflection coefficient between drain and sources, w_s is surface potential and $F_{-1/2}(x)$ is the Fermi integral function. Other symbols have the meaning as well known. After obtaining ΔU_G , $E_{n_\phi, n_r}^q(\Delta U_G)$ and $w_s(\Delta U_G)$ in cross section of channel can be calculated. Hence we can obtain the drain current by using Landauer's formula^[4].

Analytical Method

We can now calculate ΔU_G by using approximation of the Fermi integral function^[5]. For high drain bias, the second term in formula (1) including V_{DS} can be neglected when doing analytic calculations. Hence the Fermi integral function can be approximated as zero and root function in subthreshold and strong inversion region respectively^[5]. When only considering the lowest subband, ΔU_G is one of the solutions of quadratic equation, denoted as $\Delta U_G^{(1)}$ in strong inversion region. Since we can use $\Delta U_G^{(1)}$ to obtain $w_s(\Delta U_G^{(1)})$ and $E_{n_\phi, n_r}^q(\Delta U_G^{(1)})$, the drain current can be represented by Landauer's formula analytically. There by, the SPICE simulation can be carried out by using this analytic compact model including the lowest subband. Moreover when considering two subbands, ΔU_G can be represented by one of the solutions of quartic equation, denoted as $\Delta U_G^{(2)}$. However, when the gate voltage is small, the solutions of quartic equation become complex numbers, so $\Delta U_G^{(2)}$ cannot be represented analytically in weak inversion region. Therefore, we use the quadratic equation solution $\Delta U_G^{(1)}$ for small gate voltage, and the quartic equation solution $\Delta U_G^{(2)}$ for large gate voltage. According to the expressions of ΔU_G in two regions discussed above, we can make them consistent into one formula as follows:

$$\begin{aligned} \Delta U_G &= A\Delta U_G^{(1)} + B\Delta U_G^{(2)} \\ A &= [1 + \exp[a_2(c - a_3)]]^{-1} \\ B &= [1 + \exp[-a_2(c - a_3)]]^{-1} \\ c &= (V_{\text{GS}} - w_{\text{GC}} + w_{\text{FB}})/V_t - E_{n_\phi, n_r}^{q0}/k_B T, \quad (2) \end{aligned}$$

where $\Delta U_G^{(1)}$ and $\Delta U_G^{(2)}$ have been explained above, $-e\phi_{\text{GC}}$ is the work function between gate and channel materials, w_{FB} is electrostatic potential in the conduction band edge at the flat band condition, E_{n_ϕ, n_r}^{q0} is confinement energy levels of the infinite quantum well with respect to surface energy level in channel. By setting a_2 as 0.25, a_3 as 5, we can obtain a good match with this analytic model in wide device structures and bias conditions. As the same procedure considering the lowest subband, we also can carry on doing drain current calculations and HSPICE simulation

when considering two subbands.

RESULTS AND DISCUSSION

Figure 3 shows results of comparison between numerical and analytic compact model for different subband numbers. As gate voltage is becoming larger, electrons in the channel are excited to the lowest subband and the second subband to show differences between single subband and two subbands. In Figure 4, $I_{DS}-V_{GS}$ and $I_{DS}-V_{DS}$ characteristics plotted by numerical and analytic compact model considering two subbands are illustrated. They demonstrate a good agreement between the results of numerical and analytic calculations in wide device structures. Figure 5 illustrates the output characteristics of an inverter circuit simulation on HSPICE using analytic compact model with two subbands discussed above, and the drain bias is set as 1V.

CONCLUSION

An analytic compact model of quasi-ballistic and ballistic cylindrical Gate-All-Around MOSFET using perturbation method has been proposed. An analytic expression of ΔU_G using one formula in all operating region has been represented by considering two subbands, we also obtained a good agreement between our new analytic and numerical compact model. As a result, it is expected to obtain more exact agreement than considering lowest subband in strong inversion region for large-scaling model structures.

REFERENCE

- [1] T. Numata, et al. *SISPAD*, 39, 2011.
- [2] K. Natori, et al. *IEICE Trans. Electron*, VOL.E84-C, 2001.
- [3] M. Lundstrom, et al. *IEEE Trans. Electron Devices*, VOL49, NO.1, 2002
- [4] T. Numata, et al. *Jpn.J.Appl.Phys.* 49, 04DN05, 2010
- [5] A. Aymerich-Humetl et al. *J.A.P.* 54, 2850, 1983

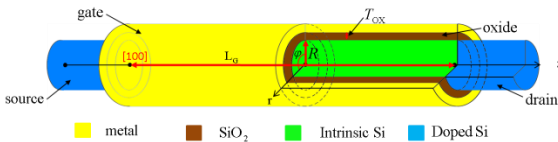


FIGURE 1. Schematic view of a cylindrical GAA-MOSFET architecture and geometrical parameters definition. The nanowire is oriented along [100] silicon lattice direction.

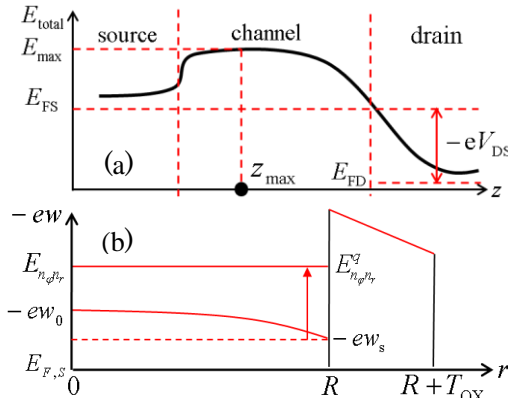


FIGURE 2 (a) Representation of energy levels of conduction band edge distribution along the z direction of channel. (b) Schematics of confinement potential energy distribution along r -component at z_{MAX} in the cross section of channel.

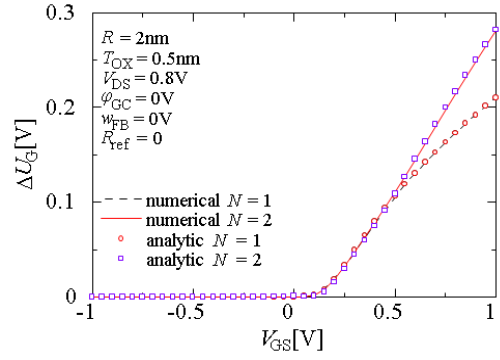


FIGURE 3. Comparison between analytic and numerical calculations for different N with one and two respectively. N is the number of subband.

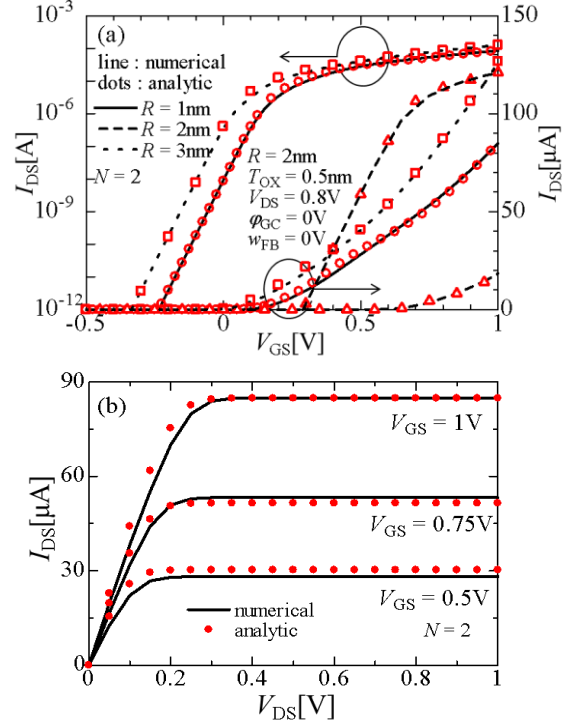


FIGURE 4. Current characteristics calculated from numerical compact model (solid line) and analytic model (dots) with wire radius from 1nm to 3nm and only 2nm in (a) $I_{DS}-V_{GS}$ and (b) $I_{DS}-V_{DS}$ characteristics respectively. N is the number of subband.

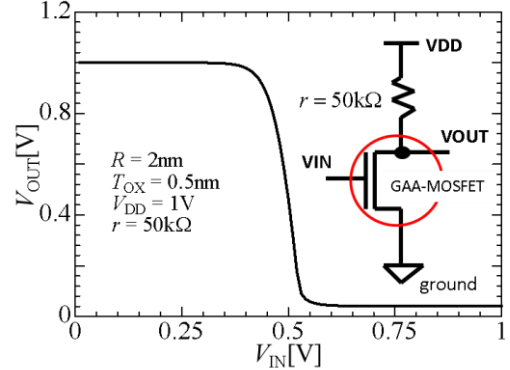


FIGURE 5. The analytic compact model of a GAA-MOSFET is introduced to HSPICE as a Verilog-A file. The output voltage V_{OUT} of the inverter circuit simulated by HSPICE simulator.